Surface-modified Wannier-Stark states in a one-dimensional optical lattice

A. Maury,* M. Donaire, M.-P. Gorza,† A. Lambrecht, and R. Guérout
Laboratoire Kastler Brossel, UPMC-Sorbonne Universités, CNRS, ENS-PSL-Research University, Collège de France; 4 place Jussieu, F-75005 Paris, France
(Received 27 June 2016; published 2 November 2016)

We study the energy spectrum of atoms trapped in a vertical one-dimensional optical lattice in close proximity to a reflective surface. We propose an effective model to describe the interaction between the atoms and the surface at any distance. Our model includes the long-range Casimir-Polder potential together with a short-range Lennard-Jones potential, which are considered nonperturbatively with respect to the optical lattice potential. We find an intricate energy spectrum which contains a pair of loosely bound states localized close to the surface in addition to a surface-modified Wannier-Stark ladder at long distances. Atomic interferometry involving those loosely bound atom-surface states is proposed to probe the adsorption dynamics of atoms on mirrors.

DOI: 10.1103/PhysRevA.94.053602

I. INTRODUCTION

Trapping and manipulating cold neutral atoms in an optical lattice offers high control over the atomic locations and robust quantum coherence on the dynamics of the atomic states. These properties make of an optical lattice an ideal system for applications in metrology [1,2] and in precision measurements of the interactions between the atoms and the environment [3]. It is to the latter that the FORCA-G project applies [4]. In particular, the FORCA-G experiment aims at performing high-precision measurements of the electromagnetic and gravitational interactions between a neutral atom and a massive dielectric surface. Ultimately, it aims at establishing accurate constraints in the search of hypothetical deviations from the Newtonian law of gravitation at short length scales, the reason why an accurate knowledge of the electromagnetic interaction is also needed. It is on the electromagnetic interaction that we concentrate in this article.

In the setup of FORCA-G atoms of ^{87}Rb are trapped in a vertical optical lattice by the potential generated by the standing waves of a laser source of wavelength $\lambda_l = 532$ nm, which reflect off a Bragg mirror (see Fig. 1). The optical potential takes the periodic form

$$V_{\mathrm{op}}(z) = U(1 - \cos 2k_l z)/2, \tag{1}$$

where $k_l = 2\pi/\lambda_l$, z is the vertical distance relative to the surface position and U is the optical depth which depends on the laser intensity. In addition, the uniform Earth gravitational field creates a linear potential

$$V_{\mathrm{g}}(z) = -mgz \tag{2}$$

with m being the atomic mass and g being the gravitational acceleration. Disregarding the atom-mirror interaction, the spectrum which results from the addition of the optical and gravitational potentials consists of a ladder of quasistable states referred to as Wannier-Stark (WS) states. The WS eigenstates are localized around the equilibrium points $z_n = n\lambda_l/2$, n being an integer, and are uniformly distributed along the energy spectrum at constant intervals $mg\lambda_l/2 = h\nu_B$. In this expression ν_B is referred to as Bloch frequency, and the degree of localization is determined by the relative optical depth with respect to the recoil energy, $U/(\hbar^2 k_l^2/2m) = U/E_r$ (see Fig. 2).

In addition to $V_{\mathrm{op}}(z)$ and $V_{\mathrm{g}}(z)$, the neutral atoms interact with the surface through the mutual coupling of their charge fluctuations to the vacuum fluctuations of the electromagnetic field. This interaction is known generically as Casimir-Polder (CP) interaction [5,6]. At zero temperature its strength depends generally on the dielectric properties of the surface, the state of the atom, and the distance between them.

The *modus operandi* of FORCA-G consists of a sequence of pulses generated by Raman lasers and microwaves which are used to create an atomic interferometer. The pulses drive the atoms through a coherent superposition of low-lying Zeeman sublevels at different lattice sites [4]. The CP interaction induces a phase shift on the atoms which depends strongly on the distance of the atoms to the surface and slightly on the internal atomic states. The phase shift accumulated by the atomic wave function throughout the sequence of pulses is finally measured by atomic interferometry techniques. If the atoms are made to oscillate between lattice sites far from the surface, the CP-induced shift is additive. Therefore, once the phase shift associated to the passage through different WS levels, which is characteristic of the interferometer scheme, is substracted, the remaining phase is the CP-induced shift we are interested in.

The latter applies to the case where the CP interaction is small with respect to the optical potential depth, so that it can be treated as a perturbation to the potential $V_{\mathrm{op}}(z) + V_{\mathrm{g}}(z)$ and hence to the original WS states. This takes place at separation distances of the order of microns, at which the perturbative development of Refs. [7,8] applies. On the contrary, at submicrometer distances and beyond the perturbative regime, it was already noticed in Ref. [7] that the CP corrections to the original WS energies diverge. This is especially relevant to the purposes of the FORCA-G project, as deviations from Newtonian gravity are expected to occur at submicrometer distances. Therefore, a precise knowledge of the CP interaction at this length scale as well as an accurate description of the spatial distribution of the atomic wave function are crucial in order to detect those gravitational effects. In Ref. [7] the authors apply a regularization scheme for the CP potential

*maury@lkb.upmc.fr
†on leave from Laboratoire de physique des lasers, Université Paris 13, Villetaneuse, France.

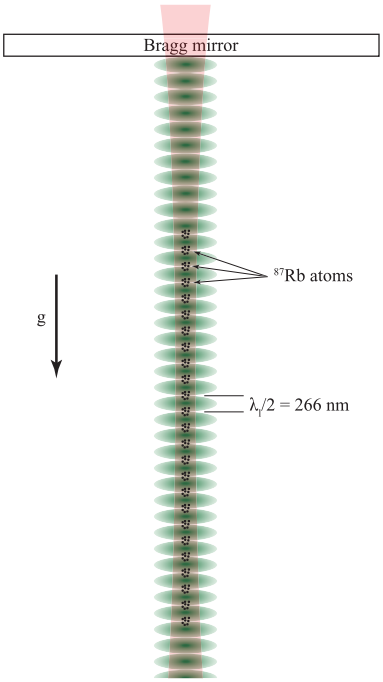

FIG. 1. Scheme of the experimental device. Cold ^{87}Rb atoms are trapped in a blue-detuned vertical optical lattice. An infrared laser at $\lambda = 1064$ nm ensures the transverse confinement. A pair of contrapropagating Raman lasers at $\lambda = 780$ nm (not shown) drives the transitions between lattice sites.

based on the assumption that the minimum distance of the atom to the surface is determined by the atomic radius. However, it is found there that the resultant corrections strongly depend on this radius. Thus, nonreliable results were obtained.

It is the main purpose of the present article to develop a nonperturbative approach to this problem in order to determine accurately the energy spectrum and the profile of the atomic states at submicrometer distances. To this end, we model the short-range interaction between the atom and the surface by a Lennard-Jones potential which features the adsorption of the atoms on the surface. We find that, in addition to slightly modified WS states, the resultant spectrum contains a number of loosely bound atom-surface states whose properties depend critically on the parameters of the Lennard-Jones potential. Nonetheless, independent measurements can be performed to determine the unknowns of such potential.

The remainder of the article is organized as follows. In Sec. II, we present the features of the potential modeling the interaction between the atom and the surface. In Sec. III we show that the overall effect of the surface leads to a complex energy spectrum significantly departing from the usual Wannier-Stark states. We conclude by calculating a typical atomic interferometry spectrum obtained using stimulated Raman transitions between those surface-modified Wannier-Stark states.

II. THE ATOM-SURFACE POTENTIAL

In addition to the optical potential described in the precedent section, the atoms interact with the mirror through

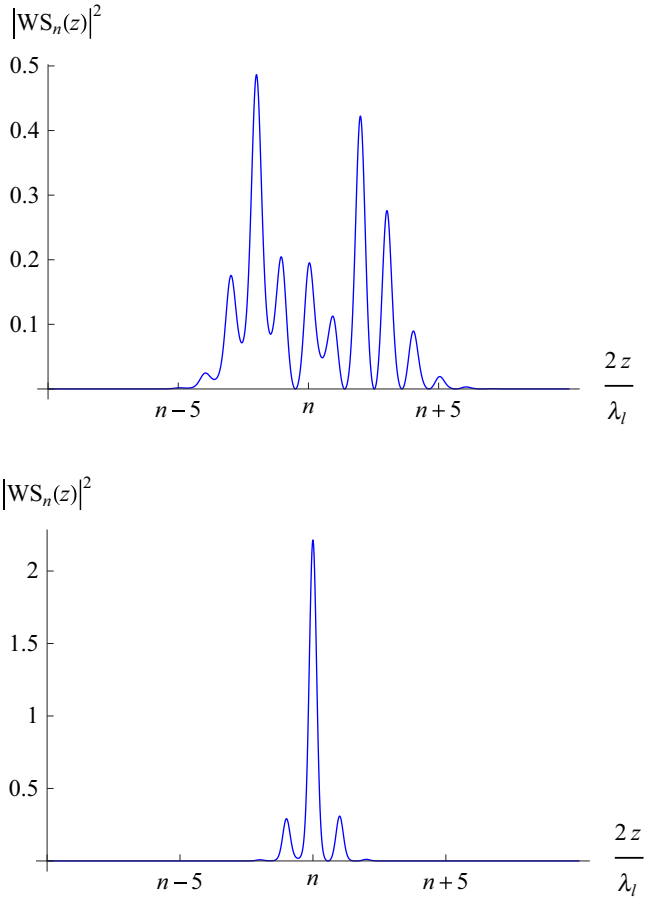

FIG. 2. Profile of the squared-norm of the wave function of the nth WS state for different values of the optical depth, $U = 3\ E_r$ (upper figure) and $U = 9\ E_r$ (lower figure).

the electromagnetic field. Quite generally, this interaction is made of two distinct components, a short-range and a long-range potentials. The short-range potential results from the spatial overlap between the electronic clouds of the atoms and the surface at subnanometer distances. In turn, this potential depends on the precise profile of the electronic density distribution, which is difficult to determine both experimentally and theoretically. Hence, a parametrization scheme is required for the short-range potential. In contrast, the long-range potential originates from the mutual coupling of the charges within the atoms and the currents in the mirror to the fluctuating electromagnetic field. This is the so-called Casimir-Polder potential, which is computed in the electric dipole approximation at second order in stationary perturbation theory.

In the framework of the scattering theory [9], the Casimir-Polder potential between a flat mirror in the (xy) plane and an atom in the ground state separated by a distance z, at temperature T, is given by [10]

$$V_{\rm s}^{\rm CP}(z) = k_B T \sum_n{}' \frac{\xi_n^2}{c^2} \frac{\alpha(i\xi_n)}{4\pi\epsilon_0} \int_0^\infty \frac{d^2\mathbf{k}}{\kappa} e^{-2\kappa z} \times \left[\rho^{\rm TE} - \left(1 + \frac{2\kappa^2 c^2}{\xi_n^2}\right)\rho^{\rm TM}\right] \quad (3)$$

with $\mathbf{k}^2 = k_x^2 + k_y^2$, $\kappa = \sqrt{\mathbf{k}^2 + \xi_n^2/c^2}$ and the sum runs over Matsubara frequencies $\xi_n = 2\pi n k_B T/\hbar$. In this equation ρ^{TE} and ρ^{TM} are the reflection coefficients of the mirror for the TE and TM polarizations, respectively, and $\alpha(i\xi)$ is the polarizability of a ^{87}Rb atom in its ground state evaluated at imaginary frequencies [11],

$$\alpha(i\xi) = \frac{2}{\hbar}\sum_j \frac{\omega_{jg} d_{jg}^2}{\omega_{jg}^2 + \xi^2}, \tag{4}$$

where $\omega_{jg} = \omega_j - \omega_g$ and d_{jg} are, respectively, the transition frequency and the electric dipole matrix element between the states $|j\rangle$ and $|g\rangle$.

Concerning the optical properties of the mirror used in the FORCA-G experiment, its design is such that it is nearly transparent at 780 nm and 1064 nm while it is reflective at 532 nm. It is a Bragg mirror formed by alternating layers of SiO_2 and Ta_2O_5. Its reflection coefficients ρ^{TE} and ρ^{TM} are obtained using standard transfer matrix theory. Let us define first by T_i the transfer matrix associated to the transmission through the interface between the layers i and $i+1$, as well as to the propagation throughout the layer $i+1$ of width d_{i+1}. It relates the field on the left of the layer i to the field on the right and reads [12]

$$T_i = \frac{1}{\bar{t}_i}\begin{pmatrix} t_i\bar{t}_i - r_i\bar{r}_i & \bar{r}_i \\ -r_i & 1 \end{pmatrix}\begin{pmatrix} e^{ik_z d_{i+1}} & 0 \\ 0 & e^{-ik_z d_{i+1}} \end{pmatrix}. \tag{5}$$

In this equation, r_i and t_i are the Fresnel amplitudes from medium i to medium $i+1$. The barred quantities are the reciprocal amplitudes from medium $i+1$ to medium i and k_z is the z component of the wave vector in medium $i+1$. The transfer matrix of the Bragg mirror, $\mathbb{T}$, is the product of the transfer matrices of all the layers $\mathbb{T} = \prod_i T_i$ and reads

$$\mathbb{T} = \frac{1}{\bar{\tau}}\begin{pmatrix} \tau\bar{\tau} - \rho\bar{\rho} & \bar{\rho} \\ -\rho & 1 \end{pmatrix}, \tag{6}$$

from which the total reflection amplitude reads $\rho = -[\mathbb{T}]_{21}/[\mathbb{T}]_{22}$.

We show in Fig. 3 the Casimir-Polder potential calculated using Eq. (3) for a temperature $T = 300$ K. The potential is scaled with z^3, the third power of the atom-surface distance, in order to emphasize the nonretarded van der Waals regime characterized by its coefficient $C_3 \approx 3.28\, a_0^3$ eV.

As for the short-range potential, we parametrize it using a $12-3$ Lennard-Jones form,[1]

$$V_{\mathrm{s}}^{\mathrm{LJ}}(z) = \frac{D}{3}\left[\left(\frac{z_0}{z}\right)^{12} - 4\left(\frac{z_0}{z}\right)^{3}\right], \tag{7}$$

which is characterized by a well depth D and an equilibrium distance z_0 which correspond to the energy and distance from the surface of an adsorbed atom, respectively. Continuity of the atom-surface potential demands that $V_{\mathrm{s}}^{\mathrm{LJ}}(z)$ and $V_{\mathrm{s}}^{\mathrm{CP}}(z)$ smoothly merge at some intermediate distance z_m. This implies

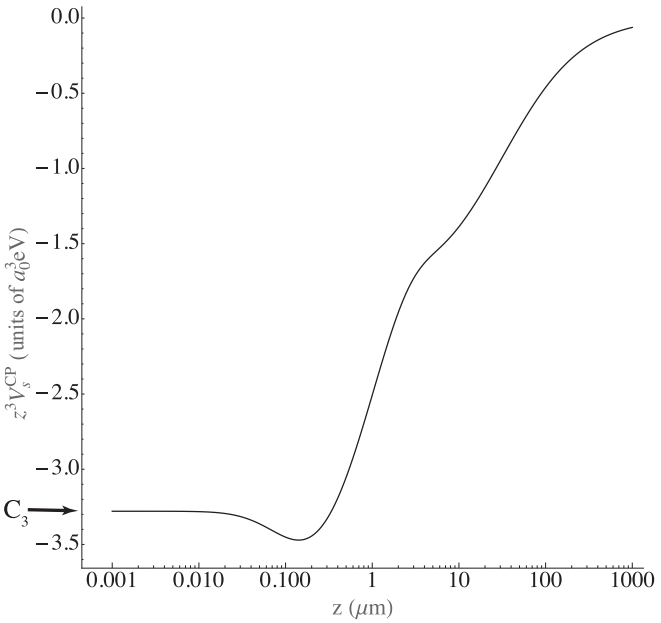

FIG. 3. The Casimir-Polder potential calculated between a Rubidium atom and a SiO_2–Ta_2O_5 Bragg mirror as a function of the distance z. The value of the van der Waals coefficient C_3 is indicated.

that D and z_0 are no longer independent but are related by the equation

$$\tfrac{4}{3} D z_0^3 = C_3, \tag{8}$$

where C_3 is the van der Waals coefficient in the Casimir-Polder potential. With this condition between the parameters D and z_0 in the Lennard-Jones potential, the matching distance z_m is chosen where both potentials $V_{\mathrm{s}}^{\mathrm{LJ}}(z)$ and $V_{\mathrm{s}}^{\mathrm{CP}}(z)$ behave in z^{-3} and leads to the total surface potential $V_{\mathrm{s}}(z)$:

$$V_{\mathrm{s}}(z) = V_{\mathrm{s}}^{\mathrm{LJ}}(z)\Theta(z_m - z) + V_{\mathrm{s}}^{\mathrm{CP}}(z)\Theta(z - z_m), \tag{9}$$

where $\Theta(z)$ is the Heaviside function.

The form used for $V_{\mathrm{s}}^{\mathrm{LJ}}(z)$ is merely of a physisorption type and hence is expected to underestimate the adsorption energy. For instance, for an equilibrium distance $z_0 = 2.3$ Å we find $D \approx 30$ meV to be compared with a value of $\approx$350 meV from a recent density functional theory calculation [13]. As a matter of fact, the parameters of the short-range potential carry the largest uncertainty in our calculation. An accurate determination of this part of the potential would require extensive *ab initio* calculations up to distances of the order of the nanometers which are beyond the scope of this work. Alternatively, the parameters D and z_0 can be determined experimentally. Be that as it may, we will study in the next section the influence of our results upon the parameters of the Lennard-Jones model.

III. SURFACE-MODIFIED WANNIER-STARK STATES

In the following and unless otherwise stated, we will refer to the distance z to the surface in units of $\lambda_l/2 = 266$ nm and the energies in units of the recoil energy $E_r = \frac{\hbar^2 k_l^2}{2m} \approx 5.37 \times 10^{-30}$ J for a Rubidium atom. The surface-modified

[1] In surface science, a $9-3$ Lennard-Jones potential is also often used as it arises as pairwise summation of $12-6$ Lennard-Jones atom-atom interactions.

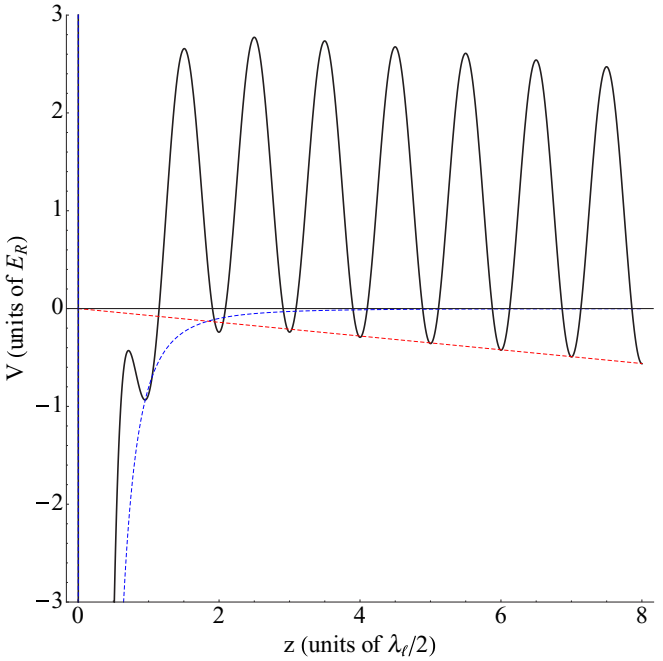

FIG. 4. Potential $V(z)$ in units of the recoil energy E_r shown as the black curve. The dashed blue and red curves are, respectively, the surface potential $V_s(z)$ and the gravitational potential $-mgz$.

Wannier-Stark states (SMWSSs) are solutions of the time-independent Schrödinger equation

$$-\frac{\hbar^2}{2m}\frac{d^2\psi_n(z)}{dz^2} + V(z)\psi_n(z) = E_n\psi_n(z), \tag{10}$$

$$\text{with } V(z) = V_s(z) + V_g(z) + V_{op}(z). \tag{11}$$

In the situation where the mirror is *above* the atoms, the potential $V(z)$ is not bounded from below so that all states are rigorously Siegert states [14]. That corresponds to the situation where the atoms could ultimately "fall from the optical lattice." Nevertheless, it has been shown in Ref. [8] that lifetimes are of the order of 10^{14} s for the first Bloch band, and hence they can be considered stable for any experimental realization. We show in Fig. 4 the potential $V(z)$ for an optical depth $U = 3E_r$.

At $z \approx 2$, the magnitudes of the gravitational and the Casimir-Polder potentials are similar. As a result, the very first optical well is strongly influenced by the surface to the point of becoming weakly bounding. Note that the minimum of the Lennard-Jones part of the surface potential has very different orders of magnitude, both in binding energy ($D \approx 10^9 E_r$) and in equilibrium distance ($z_0 = 2.3$ Å $\approx 10^{-3}\lambda_l/2$), a reason why it does not appear in Fig. 4.

The SMWSSs $\psi_n(z)$ are conveniently characterized according to their mean distance to the surface $\langle z\rangle$:

$$\langle z\rangle = \frac{\langle\psi_n|z|\psi_n\rangle}{\langle\psi_n|\psi_n\rangle}. \tag{12}$$

We show in Table I values of the mean distance $\langle z\rangle$ and the energy intervals for the first few SMWSSs calculated for an optical depth $U = 3\ E_r$ and $z_0 = 2.3$ Å, ordered according to an increasing value of $\langle z\rangle$ (the first excited Bloch band corresponds to energies greater than the optical depth U and is therefore not trapped). The closest SMWSSs are modified very strongly by the presence of the surface, which reflects on the lack of regularity characteristic of a Wannier-Stark ladder. As $\langle z\rangle$ increases, though, we progressively recover a usual Wannier-Stark ladder spaced by the Bloch energy $h\nu_B$ and integer values of $\langle z\rangle$.

TABLE I. SMWSSs for a lattice depth $U = 3\ E_r$ ordered according to their mean distance to the surface $\langle z\rangle$. Energy intervals are given in units of E_r. Further analysis (see text) shows that surface-modified Wannier-Stark states begin at $n = 3$, while the first two states are atom-surface bound states. The last column refers to the energy intervals of an infinite potential surface (i.e., perfect surface).

n	$\langle z\rangle$	$E_n - E_{n-1}$	Perfect surface
1	0.799	$E_1 = -0.0709$	
2	1.006	+1.9690	
3	3.372	−0.5468	
4	4.268	−0.1264	−0.1371
5	4.681	−0.0934	−0.0996
6	4.746	−0.0693	−0.0804
7	5.617	−0.0579	−0.0722
8	6.881	−0.0637	−0.0703
9	7.962	−0.0679	−0.0701
10	8.985	−0.0692	−0.0701
11	9.994	−0.0696	−0.0701
12	10.998	−0.0698	−0.0701
13	12.001	−0.0700	−0.0701
14	13.002	−0.0700	−0.0701
15	14.003	−0.0700	−0.0701
16	15.003	−0.0701	−0.0701
17	16.003	−0.0701	−0.0701
⋮	⋮	⋮	⋮

For the purpose of the FORCA-G experiment, we are mostly interested in the states closest to the surface.

We show in Fig. 5 the profile of the real wave functions corresponding to the first four SMWSSs according to Table I. The probability amplitudes of the first two states exhibit very

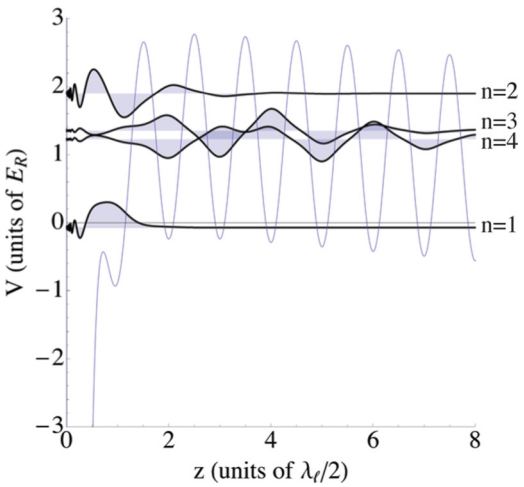

FIG. 5. Wave functions for the first four SMWSSs $\psi_n(z)$ according to Table I. As it is customary, the vertical offset of the wave functions correspond to their respective energies.

rapid oscillations within the Lennard-Jones well, while they are vanishingly small outside this well. On the other hand, the states $n = 3$ and $n = 4$ already are well spread along the optical potential as the ordinary Wannier-Stark states would. The tail of their wave functions still shows some oscillations caused by the Lennard-Jones potential.

A. Dependence upon the Lennard-Jones parameters

While modeling the short-range potential, our largest uncertainty lies in the unknown shape of the potential well. Although we have used a known analytical form which correctly converges towards the Casimir-Polder potential, the actual short-range potential may differ from the Lennard-Jones form [13]. It is therefore crucial to study the dependence of our results upon the free parameters in $V_s^{LJ}(z)$. Let us recall some general features of the bound states of a $12-3$ Lennard-Jones potential. Having a finite depth D and vanishing sufficiently fast as $z \to \infty$, the potential $V_s^{LJ}(z)$ given by Eq. (7) possesses a *finite* number of bound states. Those states represent vibrational states for an atom bound to the surface and are therefore indexed with an integer vibrational quantum number v starting with $v = 0$ for the ground state. When the total number of bound states supported by a potential well is unknown (e.g., due to uncertainties on the dissociation energy D) it is customary to label the least bound states as $v = -1$, the second least bounded states as $v = -2$, and so on. To a very good approximation, the position of the few least bound states depends only on the asymptotic behavior of the potential as $z \to \infty$ and on a noninteger effective vibrational quantum number at dissociation, v_D, which varies between 0 and -1 [15]. By decreasing continuously the depth of the potential the states $v = -1$, $v = -2$ will be eventually expelled to the continuum. From those considerations we see that, as far as the few least bound states are concerned, the exact shape of the potential energy well is not important. In our case, the effective vibrational quantum number v_D can be varied by simply decreasing the depth D of our $12-3$ Lennard-Jones model. Owing to Eq. (8), the dissociation energy D is decreased by increasing the equilibrium atom-surface distance z_0 as $D(\text{eV}) \approx 0.36 z_0^{-3}$ (Å).

We show in Fig. 6 the energies of the SMWSSs as a function of z_0 or, equivalently, as a function of decreasing dissociation energy D. In the first place, one sees that the states $n = 1$ and $n = 2$ have a very different behavior compared to all the others. The position of those states depends critically upon the dissociation energy D. As such, it is clear that the two SMWSS states $n = 1$ and $n = 2$ are basically the last two bound states $v = -2$ and $v = -1$, respectively, of the short-range potential. As the equilibrium distance z_0 increase, the energies of the states $n = 1$ and $n = 2$ increases, and they cross all the other states. Nonetheless there must be avoided crossings since all those states result from the diagonalization of the Hamiltonian operator.

On the other hand, the energies of the states starting from the $n = 3$ are very much independent of the parameters used in the short-range surface potential $V_s^{LJ}(z)$ except near an avoided crossing with a bound atom-surface state. From Fig. 6 we conclude that the state $n = 3$ can be considered the first surface-modified Wannier-Stark states. The coupling between

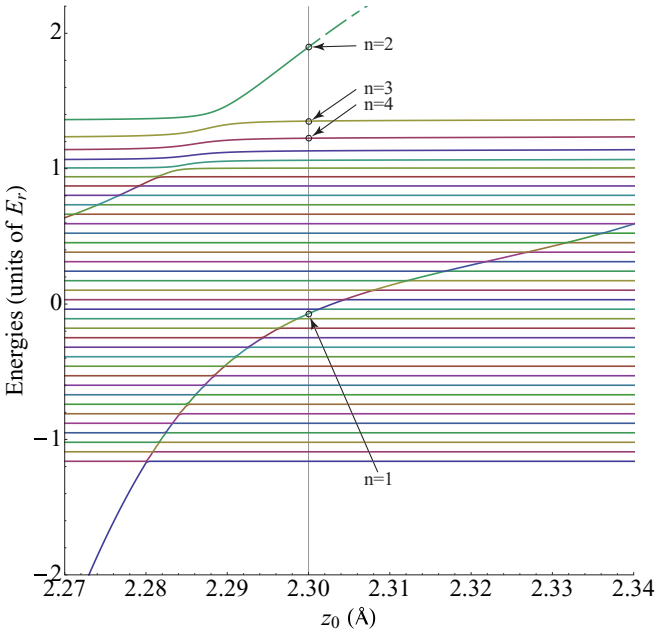

FIG. 6. Calculated energies of the SMWSSs as a function of the distance z_0 in the Lennard-Jones potential, at constant C_3 coefficient. The first four states depicted in Fig. 5 and calculated for $z_0 = 2.3$ Å are indicated by arrows.

the few first SMWSSs and the atom-surface bound states quickly vanishes as n increases owing to the vastly different mean atom-surface distance $\langle z \rangle$. This leads to negligible avoided crossings between the state $n = 2$ and already the state $n = 7$. Far from any avoided crossings, the SMWSSs are still influenced by the surface. At $z_0 = 2.3$ Å it is shown in Table I that the energy intervals between successive states are not equal to the Bloch frequency for the first Wannier-Stark states.

It is also illustrative to compare our results with those obtained from the modeling of the short-range potential with that of a perfect surface:

$$V_s(z) = \begin{cases} +\infty & z < 0 \\ 0 & z > 0 \end{cases}. \tag{13}$$

In the first place, the repulsive part of the Lennard-Jones potential plays the role of an infinite potential wall. However, in the case of an infinite potential surface the wave function has a different behavior at $z = 0$. In particular, the wave function vanishes monotically as $z \to 0$ [7,8], whereas it oscillates very rapidly within a Lennard-Jones potential. Obviously, a major drawback of an infinite potential surface is the total absence of bound atom-surface states. Values of the corresponding energy intervals can be found in Table I.

B. Simulated Raman spectrum

The experimental setup of the FORCA-G is detailed, e.g., in Ref. [16]. In it, two counterpropagating Raman lasers operating at $\lambda = 780$ nm drive coherent transitions between the ground $|5\,^2S_{1/2}, F = 1, m_F = 0\rangle$ and excited $|5\,^2S_{1/2}, F = 2, m_F = 0\rangle$ hyperfine levels of trapped ^{87}Rb atoms. Those transitions can involve different SMWSSs with a probability proportional to

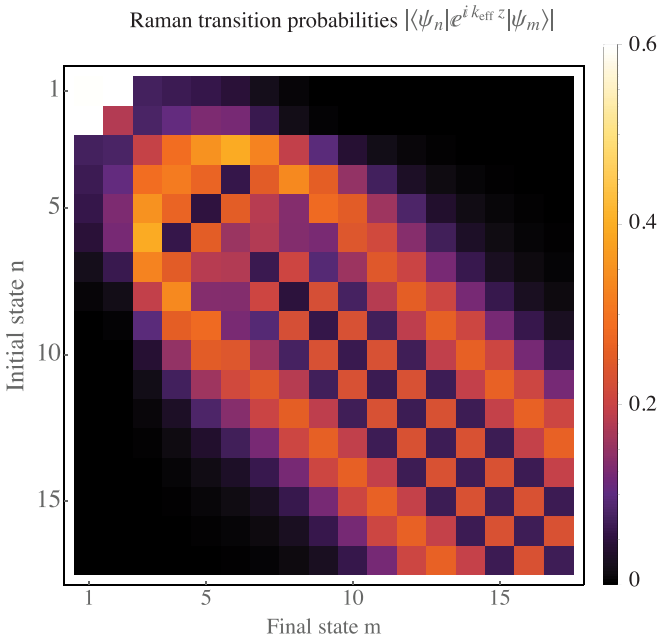

FIG. 7. Raman transition probabilities between an initial SMWSS $\psi_n(z)$ and a final state $\psi_m(z)$.

the generator of translations along the z axis, $\langle\psi_n|e^{ik_{\rm eff}z}|\psi_m\rangle$, with $k_{\rm eff} \approx 4\pi/(780\ {\rm nm})$.

We show in Fig. 7 the Raman transition probabilities between the states presented in Table I. The first two states, $\psi_1(z)$ and $\psi_2(z)$, which are the atom-surface bound states are only weakly coupled to the surface-modified Wannier-Stark states but strongly coupled to each other. We can see the smooth evolution of the SMWSSs towards "regular," unmodified Wannier-Stark states whose transition probabilities become a function of $|n-m|$ only. For a lattice depth of 3 E_r, a given state $\psi_n(z)$ roughly couples to states up to $n \pm 6$.

With a low-density atomic cloud like in Ref. [16], some 10^4 lattice sites are populated, and the Raman spectrum is dominated by transitions involving unmodified Wannier-Stark states. When the frequency difference between the two Raman lasers, $\nu_{\rm R} = \nu_{\rm R_1} - \nu_{\rm R_2}$, is scanned around the rubidium hyperfine splitting $\nu_{\rm HFS}$, this leads to a simple spectrum with lines at integer numbers of the Bloch frequency $\nu_B = h^{-1} m g \lambda_l/2 \approx 568.5$ Hz. One could imagine an experiment with a much more dense atomic sample with a size of a few microns where the contribution from the SMWSSs would be visible.

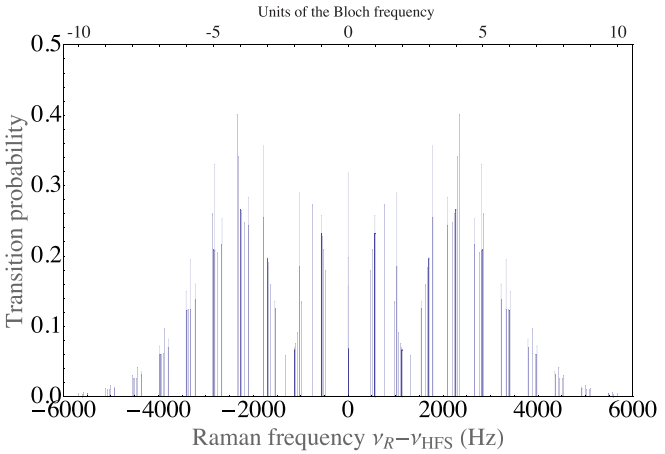

FIG. 8. Raman stick spectrum involving the states in Table I. Lines involving the atom-surface bound states $\psi_1(z)$ and $\psi_2(z)$ are not shown.

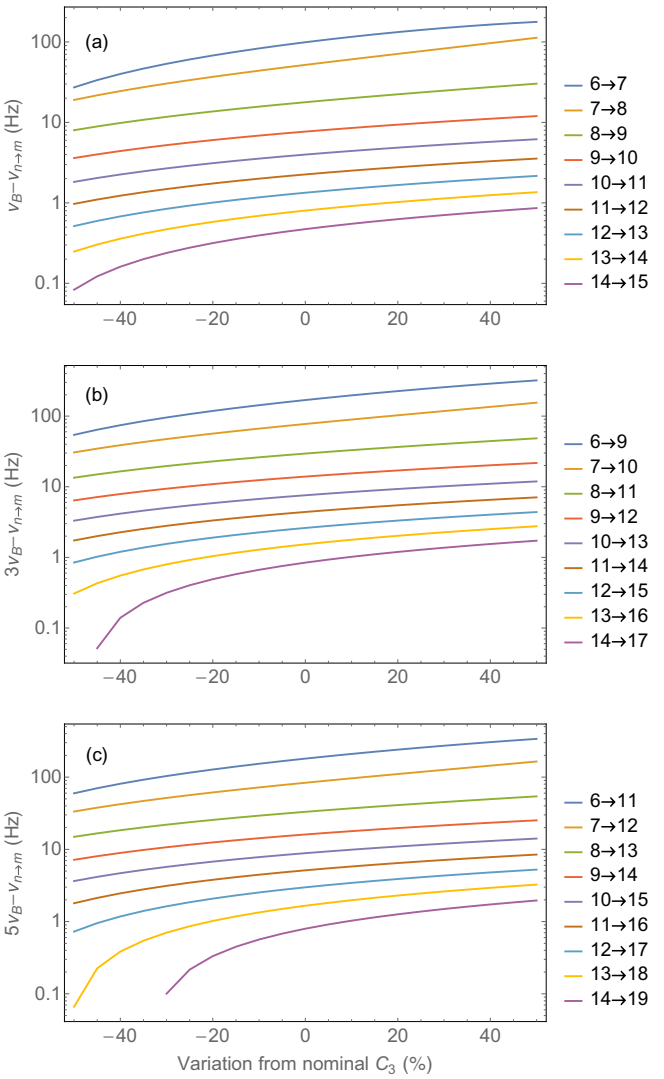

FIG. 9. Change in Raman transition frequencies $\nu_{n\to m}$, as a function of the van der Waals coefficient C_3, for selected states: (a) $|m-n| = 1$ transitions; (b) $|m-n| = 3$ transitions; (c) $|m-n| = 5$ transitions.

We show in Fig. 8 the simulated Raman stick spectrum (spectrum without line shapes) for the states listed in Table I. As we have shown in Fig. 6, the position of the atom-surface bound states $\psi_1(z)$ and $\psi_2(z)$ is largely unknown. Therefore, we do not show their contributions in the spectrum of Fig. 8. The energies of those atom-surface bound states will appear as additional lines in the Raman spectrum. As expected, the departure from the regular Wannier-Stark ladder generates many lines. Those lines have the tendency to bundle up around integer numbers of the Bloch frequency though. Recently a

relative sensibility of 4×10^{-6} at 1 s on the measure of the Bloch frequency has been demonstrated using a Ramsey-type interferometry [17]. Such a sensibility would in principle allow to resolve the lines presented in Fig. 8.

C. Determination of the Casimir-Polder potential

Up to now, the Casimir-Polder potential has been kept constant to its calculated value in Sec. II. The aim of the FORCA-G experiment is to determine this Casimir-Polder potential from a recorded Raman spectrum. Thus, we have to know how the Raman spectrum changes when one changes the Casimir-polder potential. For other references related to the use of Bloch oscillations in order to measure the coefficients in the Casimir-Polder potential, see, e.g., Refs. [18,19]. In the following, we focus on the van der Waals coefficient C_3.

We show in Fig. 9 the change in Raman transition frequencies $\nu_{n\to m} = h^{-1}(E_n - E_m)$ when the C_3 coefficient is allowed to vary from its nominal value of 3.28 a_0^3 eV calculated in Sec. II. We present in Fig. 9 selected transitions involving $|n - m| = 1$, 3, and 5 and selected states $n \geqslant 6$. A precise analysis of the position of those lines with respect to integer values of the Bloch frequency will allow the van der Waals coefficient C_3 to be determined. In fact, from an absolute uncertainty of 20 mHz [17] on the determination of Raman transition frequencies, we infer a relative uncertainty $\delta C_3/C_3$ on the van der Waals coefficient ranging from 10^{-2} to 10^{-4}.

IV. CONCLUSION

We have calculated the energies of atoms trapped in a one-dimensional vertical optical lattice taking into account the interaction between those atoms and the mirror used to realize the lattice. We have found that, in the range of energy of a few recoil energy E_r, loosely bound atom-mirror states appear as additional levels among an otherwise surface-modified Wannier-Stark ladder. The energies of those loosely bound atom-mirror states depend critically on the details of the adsorption atom-surface potential. Atomic interferometry involving those loosely bound atom-mirror states will shed light on the adsorption dynamics of rubidium atoms on mirrors. The close surface-modified Wannier-Stark states correspond to optically trapped atoms which nevertheless have a significant probability of being adsorbed by the mirror.

ACKNOWLEDGMENTS

We thank Franck Pereira dos Santos and Peter Wolf for stimulating discussions. Financial support from Agence Nationale de la Recherche ANR-10-IDEX-0001-02-PSL and ANR-13-BS04-0003-02 is gratefully acknowledged.

[1] P. Cladé, E. de Mirandes, M. Cadoret, S. Guellati-Khélifa, C. Schwob, F. Nez, L. Julien, and F. Biraben, Determination of the Fine Structure Constant Based on Bloch Oscillations of Ultracold Atoms in a Vertical Optical Lattice, Phys. Rev. Lett. **96**, 033001 (2006).

[2] M. Takamoto, F.-L. Hong, R. Higashi, and H. Katori, An optical lattice clock, Nature (London) **435**, 321 (2005).

[3] F. Impens, C. Ccapa Ttira, R. O. Behunin, and P. A. Maia Neto, Dynamical local and nonlocal Casimir atomic phases, Phys. Rev. A **89**, 022516 (2014).

[4] P. Wolf, P. Lemonde, A. Lambrecht, S. Bize, A. Landragin, and A. Clairon, From optical lattice clocks to the measurement of forces in the Casimir regime, Phy. Rev. A **75**, 063608 (2007).

[5] H. B. G. Casimir and D. Polder, The influence of retardation on the London-van der Waals forces, Phys. Rev. **73**, 360 (1948).

[6] E. M. Lifschitz, The theory of molecular attractive forces between solids, Sov. Phys. **2**, 73 (1956).

[7] R. Messina, S. Pelisson, M.-C. Angonin, and P. Wolf, Atomic states in optical traps near a planar surface, Phys. Rev. A **83**, 052111 (2011).

[8] S. Pelisson, R. Messina, M. C. Angonin, and P. Wolf, Lifetimes of atoms trapped in an optical lattice in proximity of a surface, Phys. Rev. A **88**, 013411 (2013).

[9] A. Lambrecht, P. A. Maia Neto, and S. Reynaud, The Casimir effect within scattering theory, New J. Phys. **8**, 243 (2006).

[10] G. Dufour, A. Gérardin, R. Guérout, A. Lambrecht, V. V. Nesvizhevsky, S. Reynaud, and A. Yu Voronin, Quantum reflection of antihydrogen from Casimir potential above matter slabs, Phys. Rev. A **87**, 012901 (2013).

[11] A. Derevianko, S. G. Porsev, and J. F. Babb, Electric dipole polarizabilities at imaginary frequencies for hydrogen, the alkali-metal, alkaline-earth and noble gas atoms, At. Data Nucl. Data Tables **96**, 323 (2010).

[12] G.-L. Ingold and A. Lambrecht, Casimir effect from a scattering approach, Am. J. Phys. **83**, 156 (2015).

[13] J. A. Sedlacek, E. Kim, S. T. Rittenhouse, P. F. Weck, H. R. Sadeghpour, and J. P. Shaffer, Electric Field Cancellation on Quartz by Rb Adsorbate-Induced Negative Electron Affinity, Phys. Rev. Lett. **116**, 133201 (2016).

[14] A. J. F. Siegert, On the derivation of the dispersion relation for nuclear reactions, Phys. Rev. **56**, 750 (1939).

[15] R. J. LeRoy and R. B. Bernstein, Dissociation energy and long-range potential of diatomic molecules from vibrational spacings of higher levels, J. Chem. Phys. **52**, 3869 (1970).

[16] Q. Beaufils, G. Tackmann, X. Wang, B. Pelle, S. Pelisson, P. Wolf, and F. Pereira dos Santos, Laser Controlled Tunneling in a Vertical Optical Lattice, Phys. Rev. Lett. **106**, 213002 (2011).

[17] A. Hilico, C. Solaro, M.-K. Zhou, M. Lopez, and F. Pereira dos Santos, Contrast decay in a trapped-atom interferometer, Phys. Rev. A **91**, 053616 (2015).

[18] I. Carusotto, L. Pitaevskii, S. Stringari, G. Modugno, and M. Inguscio, Sensitive Measurement of Forces at the Micron Scale using Bloch Oscillations of Ultracold Atoms, Phys. Rev. Lett. **95**, 093202 (2005).

[19] F. Sorrentino, A. Alberti, G. Ferrari, V. V. Ivanov, N. Poli, M. Schioppo, and G. M. Tino, Quantum sensor for atom-surface interactions below 10 μm, Phys. Rev. A **79**, 013409 (2009).